Original Article

MOLECULAR METABOLISM

Noggin depletion in adipocytes promotes obesity in mice

Ana M. Blázquez-Medela [1], Medet Jumabay [1], Prashant Rajbhandari [5], Tamer Sallam [1], Yina Guo [1], Jiayi Yao [1], Laurent Vergnes [5], Karen Reue [5], Li Zhang [1], Yucheng Yao [1], Alan M. Fogelman [3], Peter Tontonoz [4], Aldons J. Lusis [1,5,6], Xiuju Wu [1,], Kristina I. Boström [1,2,*,7]**

ABSTRACT

Objective: Obesity has increased to pandemic levels and enhanced understanding of adipose regulation is required for new treatment strategies. Although bone morphogenetic proteins (BMPs) influence adipogenesis, the effect of BMP antagonists such as Noggin is largely unknown. The aim of the study was to define the role of Noggin, an extracellular BMP inhibitor, in adipogenesis.

Methods: We generated adipose-derived progenitor cells and a mouse model with adipocyte-specific *Noggin* deletion using the *Adiponectin* ^{Cre} transgenic mouse, and determined the adipose phenotype of Noggin-deficiency.

Results: Our studies showed that Noggin is expressed in progenitor cells but declines in adipocytes, possibly allowing for lipid accumulation. Correspondingly, adipocyte-specific *Noggin* deletion *in vivo* promoted age-related obesity in both genders with no change in food intake. Although the loss of Noggin caused white adipose tissue hypertrophy, and whitening and impaired function in brown adipose tissue in both genders, there were clear gender differences with the females being most affected. The females had suppressed expression of brown adipose markers and thermogenic genes including peroxisome proliferator activated receptor gamma coactivator 1 alpha (PGC1alpha) and uncoupling protein 1 (UCP1) as well as genes associated with adipogenesis and lipid metabolism. The males, on the other hand, had early changes in a few BAT markers and thermogenic genes, but the main changes were in the genes associated with adipogenesis and lipid metabolism. Further characterization revealed that both genders had reductions in VO_2, VCO_2, and RER, whereas females also had reduced heat production. Noggin was also reduced in diet-induced obesity in inbred mice consistent with the obesity phenotype of the Noggin-deficient mice.

Conclusions: BMP signaling regulates female and male adipogenesis through different metabolic pathways. Modulation of adipose tissue metabolism by select BMP antagonists may be a strategy for long-term regulation of age-related weight gain and obesity.

Keywords Noggin; Bone morphogenetic protein; Adipocyte; Adipogenesis; Obesity

1. INTRODUCTION

Approximately two-thirds of the adult American population suffer from overweight or obesity, which is closely linked to adipose-tissue dysfunction and inflammation, type 2 diabetes, insulin resistance and cardiovascular disease [1,2]. There are at least two types of adipose tissue in mammals [3–5]: white adipose tissue (WAT), which has a central role in energy storage, hormone production and organ protection, and brown adipose tissue (BAT), which is highly vascularized and dissipates energy in the form of heat. BAT is considered to play an important role in the depletion of excess calories and may have a mitigating effect on cardiovascular disease [6]. Recent studies have shown that WAT can transition into BAT and vice versa, phenomena that are usually referred to as "browning" and "whitening", respectively [7,8]. The adipocytes that are responsible for "browning" have been labeled either "beige" or "brite" (brown-in-white) adipocytes [9,10]. The classical brown precursor cells derive from the dermatomyotome that express Engrailed and Myf5, whereas the beige/brite adipocytes emerge in WAT, which derive from pluripotent mesodermal stem cells [4,5]. In addition, both types of adipocytes have been traced

[1]Division of Cardiology, David Geffen School of Medicine at UCLA, Los Angeles, CA 90095, USA [2]Molecular Biology Institute, UCLA, USA [3]Department of Medicine, David Geffen School of Medicine at UCLA, Los Angeles, CA 90095, USA [4]Pathology and Laboratory Medicine, David Geffen School of Medicine at UCLA, Los Angeles, CA, USA [5]Human Genetics, David Geffen School of Medicine at UCLA, Los Angeles, CA, USA [6]Microbiology, Immunology, and Molecular Genetics, David Geffen School of Medicine at UCLA, Los Angeles, CA, USA

[7] Lead contact.

*Corresponding author. Division of Cardiology, David Geffen School of Medicine at UCLA, Box 951679, Los Angeles, CA 90095-1679, USA. Fax: +310 206 9133. E-mail: kbostrom@mednet.ucla.edu (K.I. Boström).

**Corresponding author. Division of Cardiology, David Geffen School of Medicine at UCLA, Box 951679, Los Angeles, CA 90095-1679, USA. Fax: +310 206 9133. E-mail: xiujuwu@mednet.ucla.edu (X. Wu).

Received December 7, 2018 • Revision received March 30, 2019 • Accepted April 2, 2019 • Available online 10 April 2019

https://doi.org/10.1016/j.molmet.2019.04.004

Abbreviations

Adipoq	adiponectin
aP2	adipocyte protein 2
ASC	adipose stromal cell
ALK	activin receptor-like kinase
Cdh5	cadherin 5, VE-cadherin
BAT	brown adipose tissue
BMI	body mass index
BMP	bone morphogenetic protein
CD	cluster of differentiation
Cebpa	CCAAT/enhancer-binding protein alpha
Cox	cytochrome c oxidase
Cpt1a/Cpt1b	carnitine palmitoyltransferase 1A/1B
CT	computed tomography
CV2	crossveinless 2
DAPI	4′,6-diamidino-2-phenylindole
DFAT cells	dedifferentiated fat cells
Dio2	iodothyronine deiodinase 2
DMEM	Dulbecco's modified Eagle's Medium
EE	energy expenditure
Elovl	ELOVL fatty acid elongase
ERa	estrogen receptor alpha
Fabp4	fatty acid-binding protein
FACS	fluorescence-activated cell sorting
FASN	fatty acid synthase
^{18}F-FDG	^{18}F-fludeoxyglucose
FITC	fluorescein isothiocyanate
F, Fl	flox
GAPDH	glyceraldehyde-3-phosphate dehydrogenase
HF/HS	high-fat/high-sucrose
HOMA-IR	insulin resistance index
HMDP	hybrid mouse diversity panel
HSL	hormone-sensitive lipase
ICAM	intercellular adhesion molecule
ID	inhibitor of DNA binding
IL	interleukin
MGP	matrix Gla protein
Nog	noggin
OCR	oxygen consumption rate
Oct	octamer-binding transcription factor
p	phosphorylated, phospho
PBS	phosphate-buffered saline
PE	phycoerythrin
PET	positron emission tomography
PGC1a	peroxisome proliferator activated receptor gamma coactivator 1 alpha
PRDM16	PR domain-containing 16
RER	respiratory exchange ratio
SCD1	stearoyl-CoA desaturase-1
Slc27a2	solute carrier family 27 member2
SMAD	transcription factors with homology to the *Caenorhabditis elegans* SMA and *Drosophila* MAD family of genes
TCF21	transcription factor 21
TGFβ	transforming growth factor β
UCP1	uncoupling protein 1
VCAM-1	vascular cell adhesion protein 1
VO2	oxygen consumption
WAT	white adipose tissue
WB	washing buffer
Zic1	Zic family member 1

from progenitor cells in perivascular areas, and even the vascular endothelium [11,12].

The bone morphogenetic proteins (BMPs) are part of the transforming growth factor β (TGFβ) superfamily, and regulate development and tissue differentiation through their influences on cell proliferation, lineage and migration [13,14]. The best known functions of the members of the BMP subfamily are related to bone and cartilage formation, but many BMPs are also involved in the development and pathophysiology of other organs, including the cardiovascular system [15,16], nervous system [17], kidneys [18], lungs [19] and adipose tissue [5,20]. During development, gradients of BMPs and BMP inhibitors are established and help specify cell differentiation in tissue formation [21]. Analogously, niches with 'hot spots' of high local BMP concentrations may exist in various tissues. For example, perivascular niches have been described where endothelial responses to circulating factors are transmitted to adipogenic progenitor cells [22].

BMP2 and BMP4 have been reported to stimulate white adipogenesis, whereas BMP4 and BMP7 are essential in the induction of brown adipogenesis [20,23–26]. Roles for BMP4 and BMP7 have also been described in the browning and whitening of adipose tissue [23,24,27]. BMP8b may have a role in modulating thermogenesis in BAT [28] and adrenergic-induced remodeling of the adipose neuro-vascular network [29]. It has also been described that the absence of the activin receptor-like kinase (ALK)3 (also referred to as BMPR1A) either in cells from the *Myf5*+ lineage (brown preadipocytes) or in all adipocytes leads to a deficiency in brown fat [30]. Interestingly, BMP9, which is highly expressed in liver and circulates in plasma, has been shown to regulate enzymes involved in glucose homeostasis and to be a strong inducer of brown adipogenesis [31].

The BMP activity is frequently modulated by extracellular inhibitors such as matrix Gla protein (MGP), Noggin, and Gremlin [32–34]. However, these are secreted proteins with abilities to bind BMP2, 4, and 7 [32–35] and could therefore affect adipogenesis. However, the understanding of their roles in adipose tissue remains in large part unclear and contradictory. MGP is highly expressed in differentiating human preadipocytes [36], and is higher in omental than subcutaneous adipose tissue [37]. Noggin, however, was reported to induce adipogenesis in mesenchymal stem cells from mouse bone marrow, and to circulate at higher levels in human subjects with body mass index (BMI) > 27 [38], whereas other investigators found that Noggin reduced cell differentiation in human adipose stromal cells [39]. Gremlin has been reported to inhibit adipocyte differentiation [40,41], cause preadipocyte resistance to BMP4 and impair regulation of beige and brown adipogenesis [42].

Here we address whether the BMP inhibitor Noggin has the ability of modulating adipose tissue and obesity *in vivo* through adipocyte-specific gene deletion of the *Noggin* gene in mouse. Our findings provide evidence that Noggin is a regulator of adipose tissue, and Noggin deficiency promotes age-related whitening of BAT and white adipose hypertrophy associated with obesity.

2. METHODS

2.1. Mice

Noggin$^{flox/flox}$ (*Nog*$^{fl/fl}$) (Nog tm1.1Rmh/J, stock #016117) [43], *Adiponectin* (*Adipoq*)^{Cre} (B6; FVB-Tg(Adipoq-cre)1Evdr/J, stock #010803) [44], and *VE-cadherin* (*Cadherin5*, *Cdh5*)^{Cre} (B6.FVB-Tg(Cdh5-cre) 7Mlia/J, stock #006137) [45] were obtained from the Jackson Laboratory. All mice were on C57BL/6J background. Genotypes were confirmed by PCR [46], and experiments were performed with generations F4-F6. Littermates were used as wild type controls. All mice were fed a standard chow diet (Teklad Rodent Diet 8604, Envigo, Placentia, CA). The use of animals and all experimental procedures were reviewed and approved by the University of California Los Angeles (UCLA) Chancellor's Animal Research Committee and conducted in accordance with the animal care guideline set by UCLA. The investigation conformed to the National Research Council, *Guide for the Care and Use of Laboratory Animals, Eighth Edition* (Washington, DC: The National Academies Press, 2011).

2.2. Preparation of adipose tissue-derived progenitor cells

Dedifferentiated fat (DFAT) cells and adipose stromal cells (ASCs) were prepared from 2 g of subcutaneous WAT or interscapular BAT collected from wild type C57BL/6J mice aged 8–10 weeks, as previously described [47–49]. The DFAT cells were used after passage of the initial preparation from adipocytes, between passages 1–3, and the experiments where performed in adipogenic medium from the StemPro™ Adipogenesis Differentiation Kit (Gibco/Thermofisher Scientific, Waltham, MA). Recombinant human BMP4 and Noggin, and anti-Noggin antibodies (Cat. No. AF719) were from R&D Systems (Minneapolis, MN). The ASCs were sorted by FACS as outlined below.

2.3. Body fat determination

Whole body fat, fluids and lean muscle mass of isoflurane-anesthetized mice were determined biweekly using a Bruker Optics Minispec NMR analyzer (Billerica, MA) in accordance with the manufacturer's recommendations.

2.4. Indirect calorimetry and respiratory measurements

Energy expenditure, food intake, and ambulatory activity were determined by using the Oxymax/CLAMS Comprehensive Lab Animal Monitoring System (Columbus Instruments, Columbus, OH). Respiratory measurements were made in 20 min intervals after an initial 12 h acclimation period. Energy expenditure (EE) was calculated from oxygen consumption (VO_2) and respiratory exchange ratio (RER) using the Lusk equation, EE in cal/min $= (3.815 + 1.232 \times \text{RER}) \times VO_2$ in ml/min [50]. Statistical significance for EE measurements was determined by using 2-way-ANOVA.

2.5. Glucose tolerance test

Mice aged one year were fasted for 6 h prior to the beginning of the test. Baseline measurements of blood glucose were obtained (Optium EZ kit from Abbott, Lake Bluff, IL), and the mice were injected with 2 mg glucose (Millipore Sigma, Billerica, MA) per gram of body weight. Additional blood glucose measurements were taken at 15, 30, 60, and 90 min after the injection.

2.6. Immunofluorescence

Tissues were collected at 2 months and 1 year of age. Subcutaneous fat pads were collected in the inguinal and axillary regions (the latter corresponding to the anterior subcutaneous fat pad in [51]). Visceral fat pads were collected in the gonadal and omental regions, and brown fat was collected in the interscapular region.

Tissue sections were prepared and stained as previously described [52]. Briefly, 4 μm-sections were fixed in 4% paraformaldehyde and processed as described. For immunohistochemistry and immunofluorescence, sections were permeabilized with 0.5% Triton X-100 for 10 min, followed by 3 washes with wash buffer (WB, phosphate-buffered saline (PBS) containing 0.1% Tween-20). Non-specific antibody binding sites were blocked by incubating the sections for 30 min in blocking buffer (1% BSA, 2% goat serum and 0.5% Triton X-100 in PBS). Primary antibodies were diluted in antibody buffer (PBS containing 1% BSA, 0.5% Triton X-100), and sections were incubated for overnight at 4 °C, followed by several washes in WB. Alexa Fluor 488-conjugated (green fluorescence) or Alexa Fluor 594-conjugated (red fluorescence) secondary goat anti-chicken or goat anti-rabbit antibodies (Molecular Probes, Eugene, OR) or Streptavidin (Vector Laboratories, Burlingame, CA, USA) were applied to the sections and incubated for 60 min at room temperature. After several washes in WB and a brief equilibration of the sections in PBS, the nuclei were stained with 4′,6-diamidino-2-phenylindole (DAPI, Sigma-Aldrich, St. Louis, MO). A DAPI stock solution was diluted to 300 nM in PBS, and 300 μl of the diluted solution was added to the sections, making certain that they were completely covered. The sections were incubated for 1–5 min and rinsed several times in PBS. Staining without primary antibodies served as controls. Slides without primary antibodies were used as negative controls. Images were acquired with an inverted Nikon Eclipse Ti–S microscope (Nikon Corporation, Tokyo, Japan). We used biotinylated isolectin B4 (Vector Laboratories, Burlingame, CA), and specific antibodies for Perilipin (Cat. No. 9349S, Cell Signaling, Danvers, MA), Noggin (Cat. No. AF719, R&D Systems, Minneapolis, MN), and beta-catenin (Cat. No. ab16051, Abcam, Cambridge, MA). The preparations were mounted with Prolong™ Gold Antifade Mountant (Thermo Fisher Scientific, Canoga Park, CA). Image analysis was performed on sections stained with anti-perilipin antibodies using Wolfram Mathematica 10 (Wolfram Research, Champaign, IL). Only cells with clear cell boundaries were included in the analysis (Supplemental Fig. 1).

2.7. RNA analysis

Total RNA was isolated from tissues or cultured cells using the miRNeasy Mini kit (Qiagen, Redwood City, CA) according to the manufacturer's instructions. cDNA was obtained using the High Capacity cDNA Reverse Transcription kit from Applied Biosystems (Foster City, CA). Relative quantitative PCR was performed on a 7500 Fast Real-Time PCR System using TaqMan® Universal PCR Master Mix (both from Applied Biosystems). Primers and probes for mouse genes BMP2, BMP4, BMP7, BMP8b, Gremlin, matrix Gla protein (MGP), cross-veinless 2 (CV2), Noggin, cluster of differentiation (CD)36, CD31, CD68, Adiponectin (Adipoq), Uncoupling Protein 1 (UCP1), PR domain-containing 16 (PRDM16), octamer-binding transcription factor (Oct)3/4, transcription factor 21 (TCF21), Cidea, peroxisome proliferator activated receptor gamma coactivator 1 alpha (Pgc1a), cytochrome c oxidase polypeptide 7A1 (Cox7a1), cytochrome c oxidase subunit 8B (Cox8b), iodothyronine deiodinase 2 (Dio2), Zic family member 1 (Zic1), CCAAT/enhancer-binding protein alpha (Cebpa), ELOVL fatty acid elongase 3 (Elovl3), Elovl6, solute carrier family 27 member2 (Slc27a2), carnitine palmitoyltransferase 1A (Cpt1a), Cpt1b, interleukin 6 (IL-6), intercellular adhesion molecule 1 (ICAM-1), and vascular cell adhesion protein 1 (VCAM-1) were obtained from Applied Biosystems as part of Taqman® Gene Expression Assays. Cycle conditions were: one cycle at 50 °C for 2 min, followed by one cycle at 95 °C for 10 min,

followed by 40 cycles at 95 °C for 15 s and 60 °C for 1 min. Threshold cycles of specific cDNAs were compared to the housekeeping gene glyceraldehyde-3-phosphate dehydrogenase (GAPDH) or 18S ribosomal RNA (18S rRNA) as previously described [53].

2.8. Immunoblotting

Immunoblotting was performed as previously described [46,54]. Equal amounts of tissue protein were used. Blots were incubated with specific antibodies to UCP1 (1:1,000 dilution; Cat. No. ab10983, Cell Signaling Technology) or phospho-SMAD1/5 (Ser463/465) (41D10) (1:1,000 dilution; Cell Signaling Technology, Cat. No. #9516), total SMAD (1:1,000 dilution; Santa Cruz Biotechnology, sc-7153), beta-actin (1:2,000 dilution; Sigma-Aldrich, Cat. No. A2228), hormone-sensitive lipase (HSL) (1:1,000 dilution; Cell Signaling Technology, Cat. No. 4107), phospho-HSL (Ser660) (1:1,000 dilution; Cell Signaling Technology, Cat. No. 4126), fatty acid synthase (FASN) (1:1,000 dilution; Cell Signaling Technology, Cat. No. #3180), and stearoyl-CoA desaturase-1 (SCD1) (0.2 μg/ml; Santa Cruz Biotechnology, Cat. No. sc-14719).

2.9. Fluorescence-activated cell sorting (FACS)

FACS was performed as previously described [55], and used to sort freshly isolated ASCs into CD34−CD31−, CD34+CD31−, CD34+CD31+, and CD34−CD31+ cell fractions using fluorescein isothiocyanate (FITC)-conjugated antibodies against CD34 (1:200; Cat. No. 11-0341-85, eBioscience, San Diego, CA) or phycoerythrin (PE)-conjugated antibodies against mouse CD31 (1:200; Cat. No. 561073, BD Biosciences Pharmingen). Nonspecific fluorochrome- and isotype-matched IgGs (BD Pharmingen) served as controls. Flow cytometer gates were set using unstained cells and the isotype-matched controls. Cells were gated by forward scatter (FSC) versus side scatter (SSC) to eliminate debris. A region was established to define positive PE/AF-488 fluorescence using a PE/AF-488-conjugated isotype-specific control. The number of cells stained positive for a given marker was determined by the percentage of cells present within a gate, which was established such that fewer than 2% of positive events represented nonspecific binding by the PE/AF-488-conjugated isotype-specific control. Minimums of 10,000 events were counted for each analysis. All FACS analyses were performed using a BD LSR II flow cytometer (BD Biosciences). FACS files were exported and analyzed using BD Cellquest software v.3.3.

2.10. Oil Red O staining

For Oil Red O staining, cells that were seeded at 70% confluency and treated as indicated in the text. The staining was performed using standard methods. To stain isolated adipocytes, floating adipocytes were collected in a new tube and AdipoRed (Lonza Biosciences, Walkersville, MD) diluted1:50 was added together with DAPI diluted 1:200 and incubated at room temperature for 20 min with soft shaking. The adipocytes were washed once more with PBS before mounting the preparation.

2.11. Brown fat activity

The experiments were performed in sub-thermoneutral conditions (20 °C) and after cold treatment at 4 °C as previously described [56]. Animals of two months and one year of age received one injection of approximately 70 μ Cu of ^{18}F-Fludeoxyglucose (FDG) via the tail vein. A 1-h interval for uptake was allowed between probe administration and micro-positron emission tomography (micro-PET)/micro-computed tomography (micro-CT) scanning. Image acquisition and reconstruction were performed as previously described [57]. Briefly, mice were placed in a dedicated imaging chamber designed for use for the CT and both PET systems. Data were acquired by using a Genisys 8 PET/CT (Sofie Biosciences, Culver City, CA) for 10 min and a MicroCAT II small-animal CT scanner (Siemens ImTek Inc. Knoxville, TN) for 8 min. Micro-PET images were reconstructed by using statistical maximum a posteriori probability algorithms (MAP) into multiple frames. Micro-CT Images were reconstructed using filtered back-projection without scatter or attenuation correction. We chose a ramp filter with a cutoff frequency of 0.5 and a zoom of 5 to give a voxel size of 0.379 mm^3. PET and CT Images were analyzed using Amide Software (version 1.16).

2.12. Respiratory rate measurement

The oxygen consumption rate (OCR) in fat pads was measured with an XF24 Analyzer (Seahorse Bioscience) as described [58]. Briefly, freshly isolated brown and white adipose tissues were minced and rinsed in cold PBS, placed in a Seahorse Islet Capture Microplate (3−5 mg per well), and incubated with 625 μl of unbuffered Dulbecco's Modified Eagle Medium (DMEM) (containing 2.5 mM glucose). OCR was measured before and after the injection of 200 μM etomoxir. The etomoxir-sensitive respiration represents the beta-oxidation. Experiments were triplicated; differences were tested by two-way ANOVA.

2.13. The hybrid mouse diversity panel (HMDP)

HMDP data was analyzed from 95 inbred mouse strains fed a standard chow diet and 110 inbred strains fed a high-fat/high sucrose diet for 8 weeks as previously described [59−61]. Gene expression comparisons were analyzed in 75 overlapping strains from two HMDP studies using global gene expression in epididymal adipose tissue in male mice. The correlations of gene expression and phenotypic data were calculated with the biweight midcorrelation using R package WGCNA.

2.14. Statistical analysis

Data were analyzed for statistical significance by two-way ANOVA with post hoc Tukey's analysis or multiple t test with Holm−Sidak correction for multiple comparisons using GraphPad Prism® 6.0 software (GraphPad Software, San Diego, CA). Unpaired student's t test was used for single variable comparison between two groups. Data are presented as mean ± SEM. p-values less than 0.05 were considered statistically significant. All experiments were repeated a minimum of three times.

3. RESULTS

3.1. Noggin as a potential regulator of adipose tissue

To examine the potential role of BMP inhibition in adipogenic differentiation, we compared the expression of BMP4 and BMP7, which are known to be associated with adipogenesis with that of Noggin, a well-established BMP inhibitor. Noggin was expressed in both WAT and BAT, as determined by qPCR (Figure 1A), and was detected by immunofluorescence in proximity of both adipocytes and CD31+ capillaries (Figure 1B). We then compared Noggin expression to that of BMP4, BMP7 and MGP, another BMP inhibitor, in the adipocytes and the different ASCs fractions. Both adipocytes and ASCs expressed Noggin. The ASCs fraction from subcutaneous WAT was sorted by FACS using antibodies to the vascular markers CD34 and CD31. White adipocytes and four ASCs fractions (82.1% CD34−CD31−, 3.4% CD34+CD31−, 2.9% CD34+CD31+, and 11.4% CD34−CD31+ cells) were analyzed by qPCR. The results revealed that the expression of BMP4, BMP7 and MGP was highest in the CD34+CD31− cells (Figure 1C), suggesting that the BMPs from these cells might trigger or

MOLECULAR METABOLISM 25 (2019) 50–63

www.molecularmetabolism.com

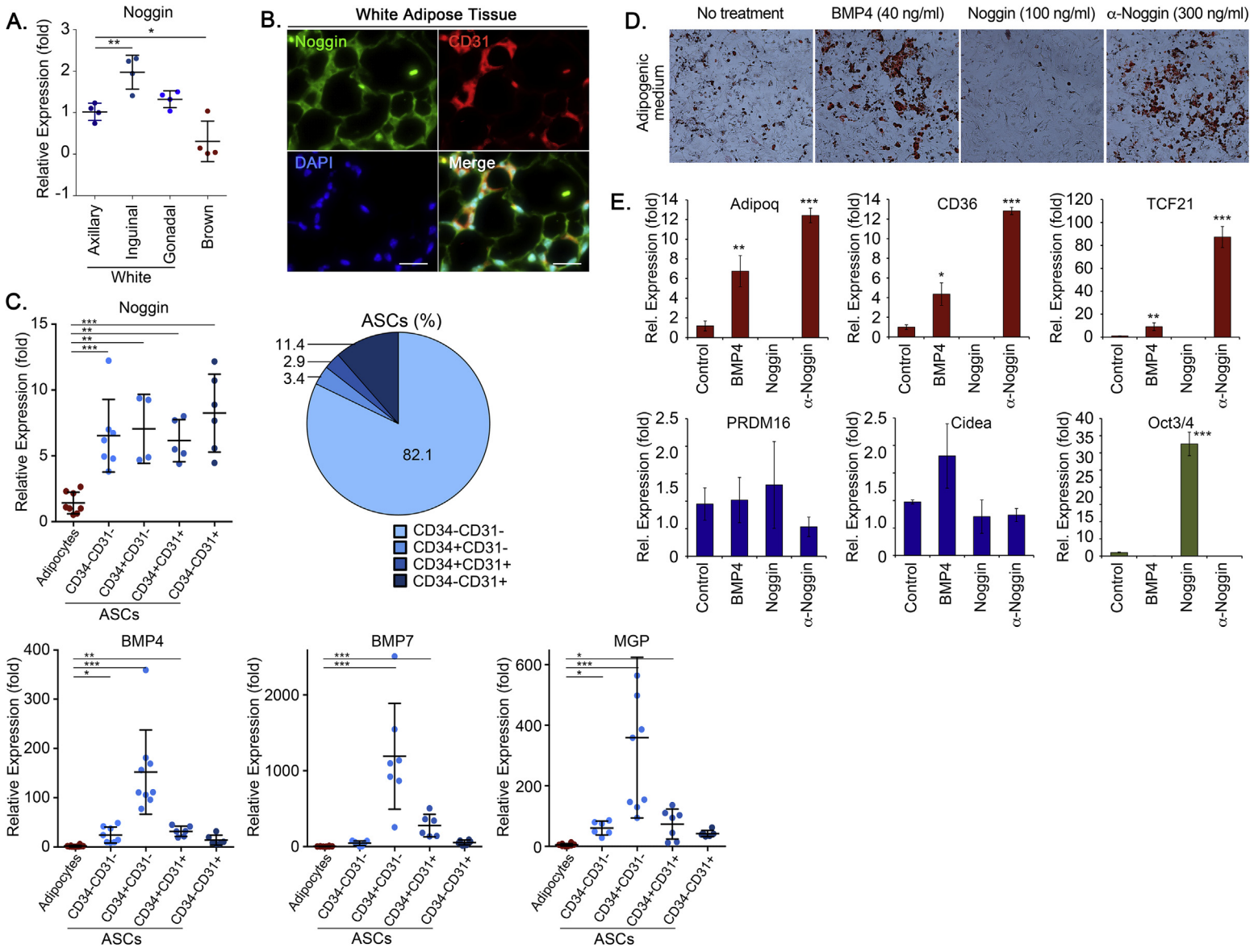

Figure 1: Noggin expression in tissue, and effect of Noggin on adipose-derived progenitor cells (DFAT cells) *in vitro*. (A) Noggin expression in white and brown fat depots compared to the axillary depot. (B) Immunofluorescence for Noggin (green) in subcutaneous WAT; co-stained with the endothelial marker CD31 (red). DAPI (blue) was used to visualize nuclei (bars, 100 μm). (C) Expression of Noggin, BMP4, BMP7 and MGP in white ASCs fractions obtained by FACS using antibodies to CD31 and CD34, compared to white adipocytes, as determined by qPCR. (D, E) DFAT cells derived from WAT were treated for 12 days with control (vehicle or non-specific IgG), BMP4, Noggin and anti-Noggin antibodies in adipogenic medium. (D) The cells were stained by Oil Red O, and (E) expression of adipogenic markers and the stem cell marker Oct3/4 was determined by qPCR. *<0.05, **<0.01, ***<0.001.

modulate adipogenic differentiation. The expression of Noggin, on the other hand, was similar in all the ASCs fractions and significantly higher than in the adipocytes (Figure 1C). Therefore, we hypothesized that decreases in Noggin allowed for lipid accumulation, a late characteristic of adipogenic differentiation.

To assess the effect of Noggin on lipid accumulation in adipogenic precursor cells *in vitro*, we cultured DFAT cells in adipogenic medium and treated the cells with control (non-specific IgG), BMP4 (50 ng/ml), Noggin (100 ng/ml) or neutralizing anti-Noggin antibodies (300 ng/ml) for 12 days. The medium was changed on days 5 and 9. The results showed that BMP4 and the anti-Noggin antibodies promoted lipid accumulation compared to control, as shown by Oil Red O staining, whereas Noggin suppressed the lipid accumulation (Figure 1D). Expression of the adipogenic markers adiponectin, Tcf21 and CD36 were consistent with the Oil Red O staining, whereas the beige/brown markers did not change significantly (Figure 1E). Interestingly, the stem cell marker Oct3/4 was enhanced in the Noggin-treated cells (Figure 1E), supporting that Noggin counteracts differentiation in these cells. Similar results were seen when treating 3T3-L1 cells, an alternative cell line (data not shown).

3.2. Noggin-deficiency promotes obesity and enlargement of lipid droplets in female and male mice

To determine the role of Noggin in adipose tissue, we generated mice with adipocyte-specific Noggin deficiency by crossbreeding $Nog^{fl/fl}$ and $Adipoq^{Cre}$ mice to obtain $Nog^{fl/fl}$;$Adipoq^{Cre}$ mice. Noggin expression in the different fat pads from these mice was significantly reduced when compared to their $Nog^{fl/fl}$ littermates, as determined by qPCR and visualized by immunofluorescence (Supplemental Figs. 2A and B). As would be expected, low levels of Noggin continued to co-localize with isolectin B4, a capillary marker, consistent with the adipocyte-specific Noggin deletion. We also generated $Nog^{fl/fl}$;$Cdh5^{Cre}$ control mice with endothelial cell-specific Noggin deficiency for comparison.

Female and male $Nog^{fl/fl}$;$Adipoq^{Cre}$ mice were allowed an *ad libitum* chow diet for up to one year, and body weight, body composition, and size of fat pads were monitored. The body weight and percent fat gradually increased and started to show significant differences at 9 and 6–9 months, respectively, compared to $Nog^{fl/fl}$ mice, as assessed by NMR (Supplemental Fig. 3). The differences were highly significant in both genders of the $Nog^{fl/fl}$;$Adipoq^{Cre}$ mice after one year (Figure 3A) when the females had nearly doubled their body weight. The muscle mass did not differ at any time point (Supplemental Fig. 3, Figure 2A). Similarly, the weight of the axillary, inguinal and gonadal fat pads, as compared to body weight, was significantly increased in females after 2 months and in both genders after one year (Supplemental Fig. 4A, Figure 2B). No differences in body weight, body composition or BAT were detected in female or male $Nog^{fl/fl}$;$Cdh5^{Cre}$ mice with the endothelial-specific Noggin loss, as compared to the $Nog^{fl/fl}$ mice (Supplemental Figs. 5A and B). Together, the results suggested that loss of Noggin in adipocytes promotes weight gain and an increase in adipose tissue with age in both genders.

Noggin provides antagonism to several BMPs, including BMP2, 4, and 7 [32] and likely BMP8b based on its close alignment with BMP7 [13]. To determine the effect of Noggin deficiency on white adipocytes, sections from the different fat pads were stained with anti-perilipin antibodies and the area of the sectioned adipocytes was determined using immunofluorescence and image analysis. Subcutaneous (axillary and inguinal) and visceral (gonadal and omental) fat pads were examined in females and males. At 2 months, only the subcutaneous adipocytes in male mice were larger in the Noggin-deficient animals (Supplemental Fig. 4B). After one year, however, adipocytes in subcutaneous fat pads as well as in the omental fat pads were significantly larger in the Noggin-deficient mice of both genders (Figure 2C). The gonadal fat pads also showed a significant enlargement in males, but not in females (Figure 2C). Again, no significant difference was detected in the $Nog^{fl/fl}$;$Cdh5^{Cre}$ mice with endothelial Noggin loss, as compared to the $Nog^{fl/fl}$ mice at one year of age (Supplemental Fig. 5C). Our results suggest that the reduced Noggin levels allowed for a potential rebalancing of the overall BMP activity that enhanced lipid accumulation with age. However, this effect was influenced by fat location and gender.

3.3. Noggin-deficiency affects BAT structure and functionality

Since Noggin is known to modulate BMP4 as well as BMP7 [32–34,62], the latter essential in brown adipogenesis, we expected that brown adipogenesis would also be affected. We examined BAT at 2 months and one year in the $Nog^{fl/fl}$;$Adipoq^{Cre}$ mice and compared to control $Nog^{fl/fl}$ mice by H&E staining and anti-perilipin immunofluorescence. This revealed that brown adipocytes in Noggin-deficient females and males had larger lipid droplets than the respective control animals at both time points (Figure 3A), suggesting that lack of Noggin promotes lipid accumulation also in brown adipocytes. It also suggested that the BAT function was altered as a result of the reduced Noggin expression. Therefore, we assessed the BAT function at 20 °C by PET at 2 months and one year of age. At 2 months, the ^{18}F-FDG uptake in BAT was less in females than in males in both types of mice, and both genders of the $Nog^{fl/fl}$;$Adipoq^{Cre}$ mice exhibited lower ^{18}F-FDG uptake than the $Nog^{fl/fl}$ control mice (Figure 3B). At one year of age, the decrease in BAT activity was more pronounced in females than in males, but the control mice continued to have higher ^{18}F-FDG uptake than the $Nog^{fl/fl}$;$Adipoq^{Cre}$ mice of the same gender (Figure 3B). The alteration in thermogenesis was confirmed by cold exposure experiments at 4 °C, which clearly showed less ^{18}F-FDG uptake in the BAT of both female and male $Nog^{fl/fl}$;$Adipoq^{Cre}$ mice at 2 months and one year of age (Figure 3C). Thus, the results suggested that the reduction in Noggin affected the BAT, and that part of the obesity in the $Nog^{fl/fl}$;$Adipoq^{Cre}$ mice might be due to the impaired BAT function.

3.4. Noggin deficiency affects metabolism and adipogenic differentiation

To investigate possible causes of the increase in adipose tissue, we analyzed metabolic differences between $Nog^{fl/fl}$;$Adipoq^{Cre}$ and $Nog^{fl/fl}$ control mice at 2 months of age using metabolic cages. This was prior to detectable differences in weight and body fat. The results showed that the $Nog^{fl/fl}$;$Adipoq^{Cre}$ mice of both genders exhibited significant decreases in VO_2, VCO_2, and RER (Figure 4A, B). The females also exhibited a decrease in heat production, which was not observed in the males (Figure 4A, B). However, there was no significant difference in the cumulative food intake between the $Nog^{fl/fl}$;$Adipoq^{Cre}$ and $Nog^{fl/fl}$ control mice of the same gender (Figure 4C, D). The food intake was measured from the time the mice were placed in the metabolic cages until the metabolic data collection was complete. In addition, no differences were detected in locomotor or ambulatory activity. On the other hand, there were significant increases in plasma levels of triglycerides and total cholesterol in the $Nog^{fl/fl}$;$Adipoq^{Cre}$ mice (Supplemental Fig. 6A). We also noted an increase in glucose and an increasing trend in insulin levels in the $Nog^{fl/fl}$;$Adipoq^{Cre}$ mice (Supplemental Fig. 6A), suggesting that the mice were developing glucose intolerance. Indeed, both genders showed evidence of glucose intolerance at 2 months of age (Figure 5D), and both genders developed histological signs of fatty liver at one year of age (Supplemental Fig. 7B).

MOLECULAR METABOLISM 25 (2019) 50–63

www.molecularmetabolism.com

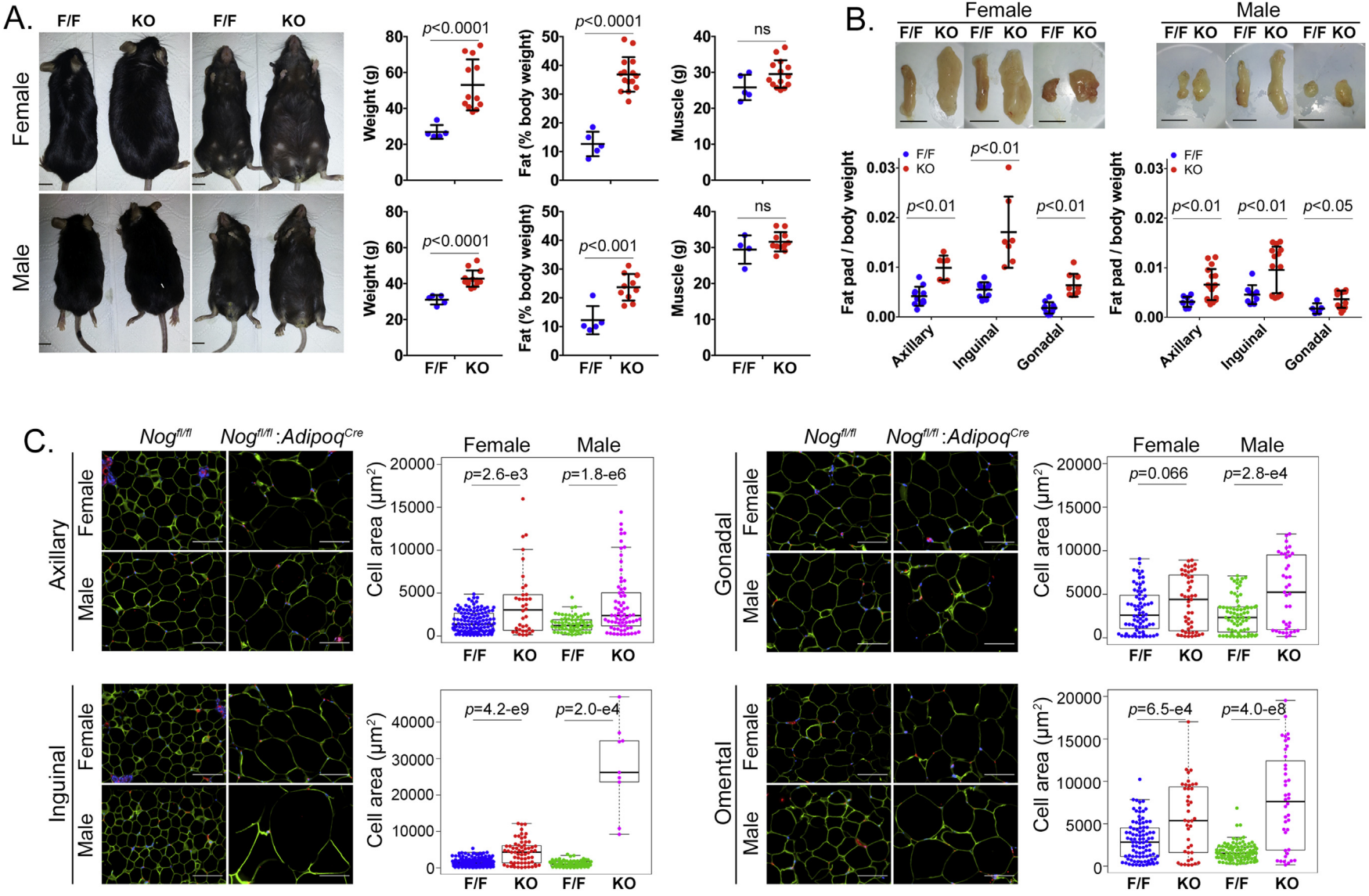

Figure 2: Adipocyte-specific deletion of Noggin in mice promotes obesity. Female and male mice with adipocyte-specific deletion of Noggin (*Nog*$^{fl/fl}$;*Adipoq*^{Cre} or KO) and control mice (*Nog*$^{fl/fl}$ or F/F) aged one year were analyzed in regards to (A) body weight and percent fat and muscle (bars, 10 mm), (B) fat pad size from the axillary, inguinal and gonadal locations (bars, 10 mm), and (C) adipocyte size as determined by cell area after immunofluorescence for Perilipin (green). Sections were co-stained for CD31 (red) and DAPI (blue) was used to visualize nuclei (bars, 100 μm).

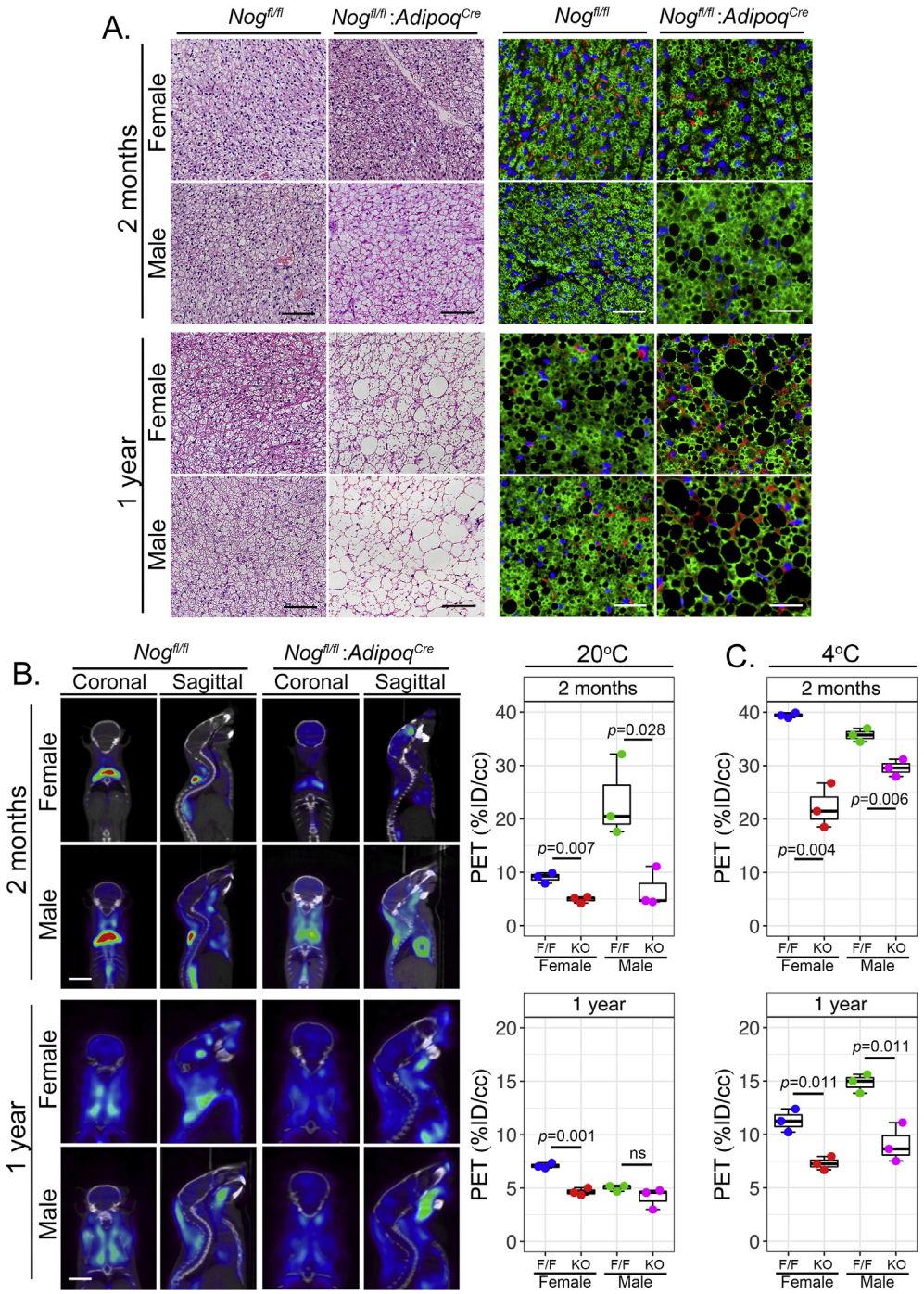

Figure 3: Adipocyte-specific deletion of Noggin impairs BAT function in mice. BAT from female and male mice with adipocyte-specific deletion of Noggin (*Nog*$^{fl/fl}$;*Adipoq*^{Cre} or KO) and control mice (*Nog*$^{fl/fl}$ or F/F) aged 2 months and one year was examined. (A) Sections of BAT were stained by H&E staining (left panels) and immunofluorescence for Perilipin (green) (right panels). Sections were co-stained for CD31 (red) and DAPI (blue) was used to visualize nuclei (bars, 100 μm). (B) ^{18}F-FDG uptake in BAT at 20 °C was visualized by PET (left panels) and subsequently quantified (right panels) (bars, 10 mm). (C) Quantification of ^{18}F-FDG uptake in BAT after cold exposure at 4 °C.

To further investigate BAT function, we first confirmed that the Noggin deletion enhanced the canonical SMAD activation in the BAT as expected. Indeed, the activation (phosphorylation) of SMAD1/5, mediators of BMP signaling, was increased in both female and male mice at 2 and 6 months of age, as determined by immunoblotting. Total SMAD, which is shown for comparison, did not change (Figure 5C, top two lanes).

We then investigated the expression by qPCR of BAT markers and thermogenic genes (PGC1a, UCP1, Cidea, Cox7a1, Cox8b, PRDM16, Dio2, and Zic1 [63]), and adipogenic and lipid metabolism regulatory genes (Cebpa, Elovl3, Elovl6, CD36, Slc27a2, Cpt1a, Cpt1b, and adiponectin). The expression was examined in BAT from mice aged 2 months and one year. The results showed that all the BAT markers and thermogenic genes decreased or showed a decreasing trend in female

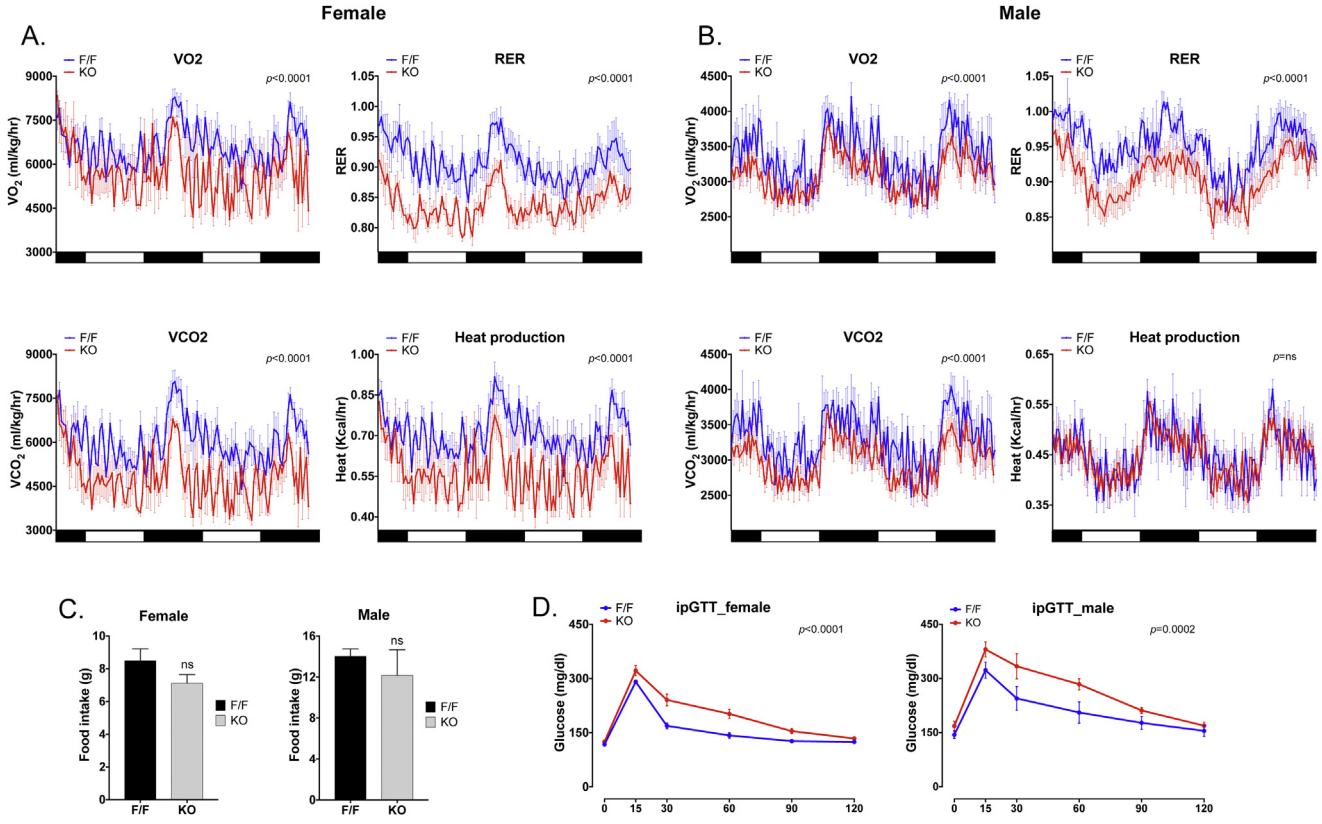

Figure 4: Adipocyte-specific deletion of Noggin in mice affects heat production, respiratory exchange ratio and oxygen consumption. Female and male mice with adipocyte-specific deletion of Noggin (*Nog*$^{fl/fl}$;*Adipoq*^{Cre} or KO) and control mice (*Nog*$^{fl/fl}$ or F/F) aged 2 months were examined in metabolic cages. (A, B) VO_2, VCO_2, RER and heat production for female (A) and male (B) mice (n = 4–6). (C) Food intake in female and male mice (n = 4–6). (D) Glucose tolerance test in female and male mice (n = 6–7). p-values are indicated in the respective panels.

Nog$^{fl/fl}$;*Adipoq*^{Cre} mice (Figure 5A), whereas only Dio2 and Zic1 showed an early decrease (at 2 months) in male *Nog*$^{fl/fl}$;*Adipoq*^{Cre} mice (Figure 5A). The decrease in UCP1 in female Noggin-deficient mice was confirmed by immunoblotting (Figure 5C). Furthermore, the adipogenic and lipid metabolism regulatory genes also decreased in the female *Nog*$^{fl/fl}$;*Adipoq*^{Cre} mice, especially after one year (Figure 5B), whereas an early increase of Cebpa, Elovl3 and Elovl6 (at 2 months) was observed in the male *Nog*$^{fl/fl}$;*Adipoq*^{Cre} mice (Figure 5B).

In addition, we investigated the expression by immunoblotting of the lipogenic genes FASN and SCD1 and the lipolytic gene HSL. Both FASN and SCD1 as well as HSL and phosphorylated (p)-HSL decreased in the female *Nog*$^{fl/fl}$;*Adipoq*^{Cre} mice (Figure 5C). Interestingly, FASN and SCD1 showed a late induction (at 6 months) without a change in HSL or p-HSL in the male Noggin-deficient males.

Thus, there were clear gender differences with the females being the most affected gender. The females showed a suppression in BAT markers and genes associated with thermogenesis, adipogenesis and lipolysis, whereas the males showed early changes in a few of the BAT markers and thermogenic genes, and then a late induction of the lipogenic genes FASN and SCD1. Together, it suggests that the BMP signaling regulates female and male adipogenesis through different metabolic pathways.

Finally we analyzed the oxygen consumption rate (OCR) in BAT from female and male *Nog*$^{fl/fl}$;*Adipoq*^{Cre} and *Nog*$^{fl/fl}$ control mice at 2 months of age, before major weight gains in the Noggin-deficient mice. The analysis showed no difference in the basal OCR in females, whereas it was decreased in the males (Figure 5D). After addition of etomoxir, an inhibitor of Cpt1a, an additional reduction in OCR was seen in the *Nog*$^{fl/fl}$;*Adipoq*^{Cre} mice, as compared to the *Nog*$^{fl/fl}$ control mice (Figure 5D), suggesting an impaired potential for beta-oxidation in Noggin-deficient BAT.

Expression of inflammatory markers, including the macrophage marker CD68, IL-6, and the adhesion molecules ICAM-1 and VCAM-1 were enhanced in BAT at one year of age in females but not in males (Supplemental Fig. 7). No change was detected in the expression of the endothelial marker CD31 (data not shown).

The differential effect of Noggin deletion on the transcriptional landscape may explain the greater obesity in the *Nog*$^{fl/fl}$;*Adipoq*^{Cre} mice females, as compared to the males. This suggests that changes in BMP signaling have gender-specific effects, and that the females are more responsive to Noggin depletion and the corresponding increase in BMP activity, especially at an early stage, which is suggested by the strong p-SMAD1/5 activation at 2 months of age (Figure 5C).

3.5. Expression of BMPs and BMP inhibitors in the HMDP

The HMDP is a collection of approximately 100 well-characterized inbred strains of mice that display a substantial diversity of metabolic phenotypes relevant to human obesity. We explored two studies in the HMDP database established by Lusis et al. [59–61,64]. First, we found that certain BMPs have relationships with obesity phenotypes, adipose expression of BMP7 in particular correlates negatively with body weight, percent fat, and insulin resistance index (HOMA-IR) (Figure 6A). We further discovered that expression of several BMP signaling components changed significantly in adipose tissue in

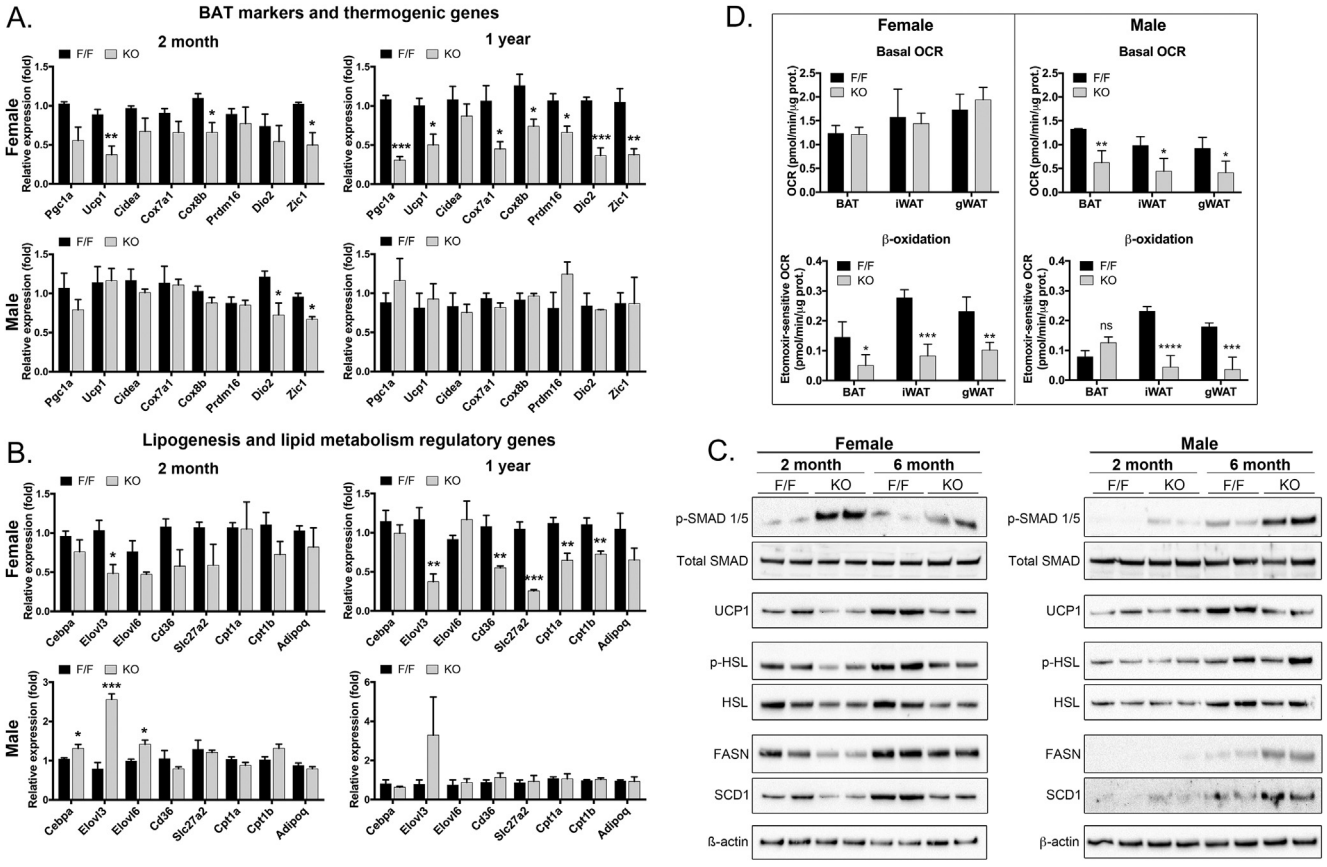

Figure 5: Adipocyte-specific deletion of Noggin affects expression of markers for adipogenic lineage, mitochondria and β-oxidation. Adipose tissues were collected from female and male mice with adipocyte-specific deletion of Noggin (*Nog*$^{fl/fl}$;*Adipoq*^{Cre} or KO) and control mice (*Nog*$^{fl/fl}$ or F/F) aged 2 months and one year. (A, B) Gene expression was determined by qPCR for (A) BAT markers and thermogenic genes, and (B) lipogenesis and lipid metabolism regulatory genes. $n = 3$; *<0.05, **<0.01, ***<0.001. (C) Gene expression was determined by immunoblotting for phosphorylated (p)-SMAD1/5 as compared to total SMAD, UCP1, p-HSL and HSL, FASN, and SCD1. Beta-actin is shown as a control. (D) Oxygen consumption rate (OCR) in BAT from female and male *Nog*$^{fl/fl}$;*Adipoq*^{Cre} and *Nog*$^{fl/fl}$ control mice in BAT at 2 months of age; basal OCR in females (top) and after addition of etomoxir (bottom). *<0.05, **<0.01, ***<0.001, ****<0.0001.

response to a high-fat/high-sucrose (HF/HS) diet as compared to chow-fed mice by microarray expression. Noggin and BMP7 both decreased and BMP2 increased, whereas BMP4 did not change significantly, although downstream BMP activity might intensify due to the lack of Noggin. In addition, the BMP type 1 receptors ALK2 and ALK3 were induced by the HF/HS diet, whereas the ALK1 and ALK6 receptors were suppressed, allowing for another level of BMP regulation (Figure 6B). Overall, the HMDP results supported that BMP modulation is important in adipose regulation.

4. DISCUSSION

Our results demonstrate that Noggin modulates BMP signaling in adipose tissue in a way that may have long-term protective actions against obesity. The results suggest that Noggin provides such protection by limiting lipid accumulation in individual adipocytes; loss of Noggin causes a "whitening" of BAT and hypertrophy of WAT through regulation of the genes for BAT differentiation and thermogenesis as well as for lipid metabolism regulatory genes. Furthermore, the effect is influenced by age and gender, and was especially pronounced in females. The impaired BAT function was detected early and preceded significant changes in the WAT.

BMP signaling is important in both morphogenesis and cell differentiation, and constellations of BMPs and BMP antagonists often act in time- and space-dependent manners during development [13,14]. The relationship between the BMPs and their antagonists can be complicated since most of the antagonists inhibit multiple BMPs each [32,33,35], and some are induced by the BMP signaling as part of feedback regulation [65]. Therefore, the removal of an inhibitor can sway the entire system rather than make a discrete change in the activity of one BMP. The BMP signaling was increased in the Noggin-deficient adipose tissue, as observed by increased the p-SMAD1/5 phosphorylation. However, we cannot with certainty link this change in SMAD activation to a specific BMP since Noggin antagonizes several BMPs including BMP4 and BMP7 [34], and possibly BMP8b due to its similarity to BMP7.

The results showed that Noggin expression was relatively stable in the sub-fractions of the ASCs, whereas that of BMP4, BMP7 and MGP was strongest in the CD34-positive cells. It is possible that Noggin is part of a temporal regulation, and functions as a barrier to activation of certain BMPs until the cells are ready for lipid accumulation. The *in vitro* results supported a negative correlation between Noggin and lipid accumulation and adipogenic differentiation, an overall opposite action to that of BMP4, at least *in vitro*. A decrease in Noggin might also

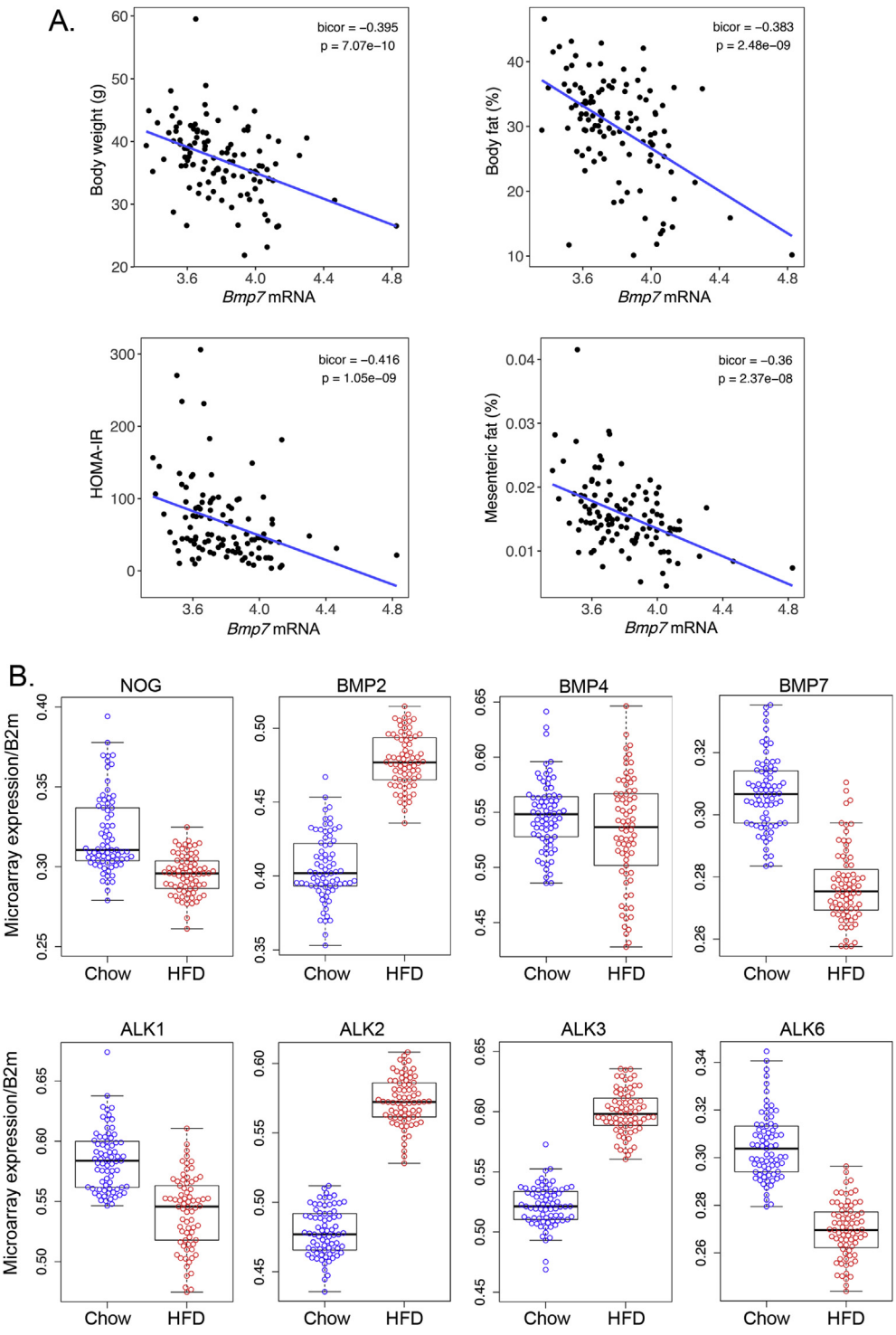

Figure 6: Adipose expression of BMP signaling components respond to high fat/high sucrose feeding in mice in the HMDP database. (A) Relationship between adipose expression of BMP7 and obesity phenotypes. (B) Expression of BMP signaling components responds to HF/HS diet compared to chow, as determined by microarray expression.

modulate the fat distribution by counteracting BMP2, which stimulates white adipogenesis and is more expressed in visceral than in subcutaneous fat depots [20]. A loss of Noggin would be less likely, however, to be due to enhanced BMP8b activity since this has been reported to increases brown adipose tissue thermogenesis [28].

When comparing our results to the HMDP database, Noggin expression is decreased in diet-induced obesity in mice from the HMDP, which would be consistent with the obesity phenotype seen in Noggin-deficient mice. BMP7 decreased in concert with Noggin, whereas BMP2 increased, suggesting that increased BMP2 activity may be

important in handling the incoming lipids. The declining BMP7 would be expected to further enhance the whitening, resulting in an association between low BMP7 levels and increased body weight, body fat, HOMA-IR and mesenteric fat.

Overall, a change in the inhibitor levels may have unexpected effects depending on the underlying BMP balance. Protein characteristics, cellular location, binding to the extracellular matrix, timing and location of expression, and varying affinities for various BMPs or BMP receptors are all aspects that can influence the role of an inhibitor. Indeed, the variety of inhibitors will make them, as a group, the perfect mediators of numerous BMP functions. For example, Noggin is a soluble protein [66] that diffuses in the tissue and contributes to tissue gradients of BMP activity. Gremlin, on the other hand, is able to form large complexes with BMP [67], while MGP is a poorly soluble protein that might immobilize BMPs in the matrix [68]. Both Gremlin and MGP are secreted by preadipocytes [36,42], but it is unclear how they differ in their BMP inhibitory function during differentiation compared to Noggin.

Our results are consistent with previous reports from Modica et al. [27] that showed that overexpression of BMP4 in brown tissue after intra-brown tissue administration of *Bmp4*-containing adenoviral vectors induced a shift to white-like phenotype in the brown adipocytes. In contrast, Qian et al. [23] demonstrated that BMP4 overexpression regulated by the fatty acid-binding protein (*Fabp4*)/adipocyte Protein 2 (*aP2*) promoter caused induction of oxidative genes and smaller lipid droplets. The use of the *aP2*-promoter has been reported to result in ectopic expression of BMP4 in multiple cells including macrophages and endothelial cells [69], which might explain the different results, especially when considering that adipocytes have been traced from endothelial cells [11].

It has been reported that the maximum size of adipocytes is around 1.0 μg of lipid per cell [70]. Here it appears that it can be exceeded in Noggin-deficient adipocytes in certain locations. Assuming that the calculated areas represent cross-sections of spherical adipocytes, the estimated size of the largest adipocytes would be in the range of 5—6 μg of lipid, i.e. 5—6-fold larger than the largest adipocyte in obese patients [70].

In our studies, the BMP signaling is affected by gender, and activated p-SMAD1/5 is higher in females at an early age. This effect may derive from gender differences in the upstream regulation of the BMP genes or in the downstream target genes, such as the inhibitor of DNA binding (ID) transcription factors. Indeed, Qian et al. [71] reported that reciprocal interactions between BMP4 and estrogen/ERa signaling could promote obesity and insulin resistance in aging female mice. These interactions could be directly targeted by Noggin through its interaction with BMP4. The findings by Grefhorst et al. [72] might also be applicable in our case. They reported that estrogen increases BMP8b expression in BAT, which might add to the effect on the BAT and the thermogenesis in the female mice. The male mice showed little difference in the thermogenic genes, but did show evidence of enhanced lipogenesis ultimately resulting in a similar phenotype.

On the transcriptional level, the ID1-4 transcription factors have been implicated in the regulation of adipogenic differentiation and development [73]. These are frequently targeted by BMP signaling. Interestingly, overexpression of ID1 in the adipose tissue results in age-associated and diet-induced obesity in mice, which has similarities to the Noggin-deficient phenotype, whereas lack of ID1 enhances the expression of UCP1 and genes associated with beige adipocytes in response to cold exposure [74]. Thus, the ID factors are likely to be important in mediating the BMP effects in adipose tissue. Altogether, the differences that arise from gender-specific differences in the Noggin-deficient mice will require further investigations.

5. CONCLUSIONS

Noggin declines in adipose progenitor cells during adipogenesis *in vitro* allowing for lipid accumulation. In a similar way, adipocyte-specific *Noggin* depletion in mice promotes age-related obesity with white adipose tissue hypertrophy in subcutaneous and omental fat pads, and whitening, reduced brown adipose function and diminished expression of PGC1alpha and UCP1. The obesity is age-related, independent of food intake, and occurs in both genders, but with reductions in heat production and expression of mitochondria and beta-oxidation markers restricted to female mice. Thus, the BMP antagonists may be essential for long-term regulation of obesity.

AUTHOR CONTRIBUTIONS

A.M.B.M. conceptualization, methodology, validation, formal analysis, investigation, data curation, writing — original draft, writing — review & editing, visualization, M.J. investigation, validation, formal analysis, P.R. investigation, formal analysis, T.S. investigation, formal analysis, Y.G. methodology, formal analysis, J.Y. investigation, formal analysis, L.V. investigation, formal analysis, K.R. investigation, formal analysis, L.Z. conceptualization, investigation, Y.Y. conceptualization, investigation, A.M.F. conceptualization, supervision, project administration, funding acquisition, P.T. conceptualization, supervision, A.J.L. conceptualization, supervision, X.W. methodology, validation, formal analysis, investigation, data curation, writing — review & editing, visualization, K.I.B. conceptualization, formal analysis, writing — original draft, writing — review & editing, visualization, supervision, project administration, funding acquisition

ACKNOWLEDGMENTS

Funding for this work was provided in part by NIH/NHLBI: grant number HL30568 (A.M.F., K.I.B., P.T., A.J.L), NIH/NHLBI: grant number HL81397 (K.I.B.), and NIH/NHLBI: grant number HL112839 (K.I.B.), and the American Heart Association: grant number 13SDG17190013 (M.J.).

CONFLICT OF INTEREST

There are no financial interests of conflicts of interest to disclose for any of the authors.

APPENDIX A. SUPPLEMENTARY DATA

Supplementary data to this article can be found online at https://doi.org/10.1016/j.molmet.2019.04.004.

REFERENCES

[1] W.H. Organization, 2017. Double-duty actions for nutrition: policy brief WHO/NMH/NHD/17, vol. 2. p. 1—12.

[2] Poirier, P., Giles, T.D., Bray, G.A., Hong, Y., Stern, J.S., Pi-Sunyer, F.X., Eckel, R.H., A. American Heart, P.A. Obesity Committee of the Council on Nutrition, Metabolism, 2006. Obesity and cardiovascular disease: pathophysiology, evaluation, and effect of weight loss: an update of the 1997 American Heart association scientific statement on obesity and heart disease from the

obesity committee of the council on nutrition, physical activity, and metabolism. Circulation 113:898–918.
[3] Cohen, P., Spiegelman, B.M., 2016. Cell biology of fat storage. Molecular Biology of the Cell 27:2523–2527.
[4] Tang, Q.Q., Lane, M.D., 2012. Adipogenesis: from stem cell to adipocyte. Annual Review of Biochemistry 81:715–736.
[5] Kajimura, S., Saito, M., 2014. A new era in brown adipose tissue biology: molecular control of brown fat development and energy homeostasis. Annual Review of Physiology 76:225–249.
[6] Kiefer, F.W., 2017. The significance of beige and brown fat in humans. Endocrine Connections 6:R70–R79.
[7] Bartelt, A., Heeren, J., 2014. Adipose tissue browning and metabolic health. Nature Reviews Endocrinology 10:24–36.
[8] Cinti, S., 2017. UCP1 protein: the molecular hub of adipose organ plasticity. Biochimie 134:71–76.
[9] Rosenwald, M., Wolfrum, C., 2014. The origin and definition of brite versus white and classical brown adipocytes. Adipocyte 3:4–9.
[10] Ishibashi, J., Seale, P., 2010. Medicine. Beige can be slimming. Science 328: 1113–1114.
[11] Tran, K.V., Gealekman, O., Frontini, A., Zingaretti, M.C., Morroni, M., Giordano, A., et al., 2012. The vascular endothelium of the adipose tissue gives rise to both white and brown fat cells. Cell Metabolism 15:222–229.
[12] Planat-Benard, V., Silvestre, J.S., Cousin, B., Andre, M., Nibbelink, M., Tamarat, R., et al., 2004. Plasticity of human adipose lineage cells toward endothelial cells: physiological and therapeutic perspectives. Circulation 109:656–663.
[13] Carreira, A.C., Alves, G.G., Zambuzzi, W.F., Sogayar, M.C., Granjeiro, J.M., 2014. Bone morphogenetic proteins: structure, biological function and therapeutic applications. Archives of Biochemistry and Biophysics 561:64–73.
[14] Wang, R.N., Green, J., Wang, Z., Deng, Y., Qiao, M., Peabody, M., et al., 2014. Bone morphogenetic protein (BMP) signaling in development and human diseases. Genes and Diseases 1:87–105.
[15] Garcia de Vinuesa, A., Abdelilah-Seyfried, S., Knaus, P., Zwijsen, A., Bailly, S., 2016. BMP signaling in vascular biology and dysfunction. Cytokine & Growth Factor Reviews 27:65–79.
[16] Morrell, N.W., Bloch, D.B., Ten Dijke, P., Goumans, M.J., Hata, A., Smith, J., et al., 2016. Targeting BMP signalling in cardiovascular disease and anaemia. Nature Reviews Cardiology 13:106–120.
[17] Hegarty, S.V., O'Keeffe, G.W., Sullivan, A.M., 2013. BMP-Smad 1/5/8 signalling in the development of the nervous system. Progress in Neurobiology 109:28–41.
[18] Nishinakamura, R., Sakaguchi, M., 2014. BMP signaling and its modifiers in kidney development. Pediatric Nephrology 29:681–686.
[19] Hines, E.A., Sun, X., 2014. Tissue crosstalk in lung development. Journal of Cellular Biochemistry 115:1469–1477.
[20] Guiu-Jurado, E., Unthan, M., Bohler, N., Kern, M., Landgraf, K., Dietrich, A., et al., 2016. Bone morphogenetic protein 2 (BMP2) may contribute to partition of energy storage into visceral and subcutaneous fat depots. Obesity 24: 2092–2100.
[21] Pera, E.M., Acosta, H., Gouignard, N., Climent, M., Arregi, I., 2014. Active signals, gradient formation and regional specificity in neural induction. Experimental Cell Research 321:25–31.
[22] Lin, G., Garcia, M., Ning, H., Banie, L., Guo, Y.L., Lue, T.F., et al., 2008. Defining stem and progenitor cells within adipose tissue. Stem Cells and Development 17:1053–1063.
[23] Qian, S.W., Tang, Y., Li, X., Liu, Y., Zhang, Y.Y., Huang, H.Y., et al., 2013. BMP4-mediated brown fat-like changes in white adipose tissue alter glucose and energy homeostasis. Proceedings of the National Academy of Sciences of the United States of America 110:E798–E807.
[24] Tseng, Y.H., Kokkotou, E., Schulz, T.J., Huang, T.L., Winnay, J.N., Taniguchi, C.M., et al., 2008. New role of bone morphogenetic protein 7 in brown adipogenesis and energy expenditure. Nature 454:1000–1004.
[25] Bowers, R.R., Lane, M.D., 2007. A role for bone morphogenetic protein-4 in adipocyte development. Cell Cycle 6:385–389.
[26] Xue, R., Wan, Y., Zhang, S., Zhang, Q., Ye, H., Li, Y., 2014. Role of bone morphogenetic protein 4 in the differentiation of brown fat-like adipocytes. American Journal of Physiology. Endocrinology and Metabolism 306:E363–E372.
[27] Modica, S., Straub, L.G., Balaz, M., Sun, W., Varga, L., Stefanicka, P., et al., 2016. Bmp4 promotes a brown to white-like adipocyte shift. Cell Reports 16: 2243–2258.
[28] Whittle, A.J., Carobbio, S., Martins, L., Slawik, M., Hondares, E., Vazquez, M.J., et al., 2012. BMP8B increases brown adipose tissue thermogenesis through both central and peripheral actions. Cell 149:871–885.
[29] Pellegrinelli, V., Peirce, V.J., Howard, L., Virtue, S., Turei, D., Senzacqua, M., et al., 2018. Adipocyte-secreted BMP8b mediates adrenergic-induced remodeling of the neuro-vascular network in adipose tissue. Nature Communications 9:4974.
[30] Schulz, T.J., Huang, P., Huang, T.L., Xue, R., McDougall, L.E., Townsend, K.L., et al., 2013. Brown-fat paucity due to impaired BMP signalling induces compensatory browning of white fat. Nature 495:379–383.
[31] Kuo, M.M., Kim, S., Tseng, C.Y., Jeon, Y.H., Choe, S., Lee, D.K., 2014. BMP-9 as a potent brown adipogenic inducer with anti-obesity capacity. Biomaterials 35:3172–3179.
[32] Umulis, D., O'Connor, M.B., Blair, S.S., 2009. The extracellular regulation of bone morphogenetic protein signaling. Development 136:3715–3728.
[33] Walsh, D.W., Godson, C., Brazil, D.P., Martin, F., 2010. Extracellular BMP-antagonist regulation in development and disease: tied up in knots. Trends in Cell Biology 20:244–256.
[34] Blazquez-Medela, A.M., Jumabay, M., Bostrom, K.I., 2019. Beyond the bone: bone morphogenetic protein signaling in adipose tissue. Obesity Reviews.
[35] Yao, Y., Jumabay, M., Wang, A., Bostrom, K.I., 2011. Matrix Gla protein deficiency causes arteriovenous malformations in mice. Journal of Clinical Investigation 121:2993–3004.
[36] Mutch, D.M., Rouault, C., Keophiphath, M., Lacasa, D., Clement, K., 2009. Using gene expression to predict the secretome of differentiating human preadipocytes. International Journal of Obesity 33:354–363.
[37] van Beek, E.A., Bakker, A.H., Kruyt, P.M., Hofker, M.H., Saris, W.H., Keijer, J., 2007. Intra- and interindividual variation in gene expression in human adipose tissue. Pflügers Archiv: European journal of physiology 453:851–861.
[38] Sawant, A., Chanda, D., Isayeva, T., Tsuladze, G., Garvey, W.T., Ponnazhagan, S., 2012. Noggin is novel inducer of mesenchymal stem cell adipogenesis: implications for bone health and obesity. Journal of Biological Chemistry 287:12241–12249.
[39] Gustafson, B., Smith, U., 2012. The WNT inhibitor Dickkopf 1 and bone morphogenetic protein 4 rescue adipogenesis in hypertrophic obesity in humans. Diabetes 61:1217–1224.
[40] Wu, Q., Tang, S.G., Yuan, Z.M., 2015. Gremlin 2 inhibits adipocyte differentiation through activation of Wnt/beta-catenin signaling. Molecular Medicine Reports 12:5891–5896.
[41] Gu, C., Xu, Y., Zhang, S., Guan, H., Song, S., Wang, X., et al., 2016. miR-27a attenuates adipogenesis and promotes osteogenesis in steroid-induced rat BMSCs by targeting PPARgamma and GREM1. Scientific Reports 6:38491.
[42] Gustafson, B., Hammarstedt, A., Hedjazifar, S., Hoffmann, J.M., Svensson, P.A., Grimsby, J., et al., 2015. BMP4 and BMP antagonists regulate human white and beige adipogenesis. Diabetes 64:1670–1681.
[43] Stafford, D.A., Brunet, L.J., Khokha, M.K., Economides, A.N., Harland, R.M., 2011. Cooperative activity of noggin and gremlin 1 in axial skeleton development. Development 138:1005–1014.
[44] Eguchi, J., Wang, X., Yu, S., Kershaw, E.E., Chiu, P.C., Dushay, J., et al., 2011. Transcriptional control of adipose lipid handling by IRF4. Cell Metabolism 13: 249–259.
[45] Alva, J.A., Zovein, A.C., Monvoisin, A., Murphy, T., Salazar, A., Harvey, N.L., et al., 2006. VE-Cadherin-Cre-recombinase transgenic mouse: a tool for

lineage analysis and gene deletion in endothelial cells. Developmental dynamics : an official publication of the American Association of Anatomists 235: 759–767.

[46] Yao, Y., Jumabay, M., Ly, A., Radparvar, M., Wang, A.H., Abdmaulen, R., et al., 2012. Crossveinless 2 regulates bone morphogenetic protein 9 in human and mouse vascular endothelium. Blood 119:5037–5047.

[47] Jumabay, M., Abdmaulen, R., Ly, A., Cubberly, M.R., Shahmirian, L.J., Heydarkhan-Hagvall, S., et al., 2014. Pluripotent stem cells derived from mouse and human white mature adipocytes. Stem Cells Translational Medicine 3: 161–171.

[48] Jumabay, M., Abdmaulen, R., Urs, S., Heydarkhan-Hagvall, S., Chazenbalk, G.D., Jordan, M.C., et al., 2012. Endothelial differentiation in multipotent cells derived from mouse and human white mature adipocytes. Journal of Molecular and Cellular Cardiology 53:790–800.

[49] Jumabay, M., Zhumabai, J., Mansurov, N., Niklason, K.C., Guihard, P.J., Cubberly, M.R., et al., 2018. Combined effects of bone morphogenetic protein 10 and crossveinless-2 on cardiomyocyte differentiation in mouse adipocyte-derived stem cells. Journal of Cellular Physiology 233:1812–1822.

[50] McLean, J.A., Tobin, G., 1987. Animal and human calorimetry. Cambridge Cambridgeshire; New York: Cambridge University Press.

[51] de Jong, J.M., Larsson, O., Cannon, B., Nedergaard, J., 2015. A stringent validation of mouse adipose tissue identity markers. American Journal of Physiology. Endocrinology and Metabolism 308:E1085–E1105.

[52] Yao, Y., Jumabay, M., Ly, A., Radparvar, M., Cubberly, M.R., Bostrom, K.I., 2013. A role for the endothelium in vascular calcification. Circulation Research 113:495–504.

[53] Bostrom, K., Zebboudj, A.F., Yao, Y., Lin, T.S., Torres, A., 2004. Matrix GLA protein stimulates VEGF expression through increased transforming growth factor-beta1 activity in endothelial cells. Journal of Biological Chemistry 279: 52904–52913.

[54] Yao, Y., Bennett, B.J., Wang, X., Rosenfeld, M.E., Giachelli, C., Lusis, A.J., et al., 2010. Inhibition of bone morphogenetic proteins protects against atherosclerosis and vascular calcification. Circulation Research 107:485–494.

[55] Matsumoto, T., Kano, K., Kondo, D., Fukuda, N., Iribe, Y., Tanaka, N., et al., 2008. Mature adipocyte-derived dedifferentiated fat cells exhibit multilineage potential. Journal of Cellular Physiology 215:210–222.

[56] Wang, X., Minze, L.J., Shi, Z.Z., 2012. Functional imaging of brown fat in mice with 18F-FDG micro-PET/CT. Journal of Visualized Experiments.

[57] Fueger, B.J., Czernin, J., Hildebrandt, I., Tran, C., Halpern, B.S., Stout, D., et al., 2006. Impact of animal handling on the results of 18F-FDG PET studies in mice. Journal of Nuclear Medicine 47:999–1006.

[58] Martin, L.J., Lau, E., Singh, H., Vergnes, L., Tarling, E.J., Mehrabian, M., et al., 2012. ABCC6 localizes to the mitochondria-associated membrane. Circulation Research 111:516–520.

[59] Bennett, B.J., Farber, C.R., Orozco, L., Kang, H.M., Ghazalpour, A., Siemers, N., et al., 2010. A high-resolution association mapping panel for the dissection of complex traits in mice. Genome Research 20:281–290.

[60] Parks, B.W., Nam, E., Org, E., Kostem, E., Norheim, F., Hui, S.T., et al., 2013. Genetic control of obesity and gut microbiota composition in response to high-fat, high-sucrose diet in mice. Cell metabolism 17:141–152.

[61] Parks, B.W., Sallam, T., Mehrabian, M., Psychogios, N., Hui, S.T., Norheim, F., et al., 2015. Genetic architecture of insulin resistance in the mouse. Cell Metabolism 21:334–346.

[62] Zhu, W., Kim, J., Cheng, C., Rawlins, B.A., Boachie-Adjei, O., Crystal, R.G., et al., 2006. Noggin regulation of bone morphogenetic protein (BMP) 2/7 heterodimer activity in vitro. Bone 39:61–71.

[63] Calderon-Dominguez, M., Mir, J.F., Fucho, R., Weber, M., Serra, D., Herrero, L., 2016. Fatty acid metabolism and the basis of brown adipose tissue function. Adipocyte 5:98–118.

[64] Lusis, A.J., Seldin, M.M., Allayee, H., Bennett, B.J., Civelek, M., Davis, R.C., et al., 2016. The hybrid mouse diversity panel: a resource for systems genetics analyses of metabolic and cardiovascular traits. The Journal of Lipid Research 57:925–942.

[65] Yao, Y., Zebboudj, A.F., Shao, E., Perez, M., Bostrom, K., 2006. Regulation of bone morphogenetic protein-4 by matrix GLA protein in vascular endothelial cells involves activin-like kinase receptor 1. Journal of Biological Chemistry 281:33921–33930.

[66] Groppe, J., Greenwald, J., Wiater, E., Rodriguez-Leon, J., Economides, A.N., Kwiatkowski, W., et al., 2002. Structural basis of BMP signalling inhibition by the cystine knot protein. Noggin Nature 420:636–642.

[67] Kisonaite, M., Wang, X., Hyvonen, M., 2016. Structure of Gremlin-1 and analysis of its interaction with BMP-2. Biochemical Journal 473:1593–1604.

[68] Price, P.A., Williamson, M.K., 1985. Primary structure of bovine matrix Gla protein, a new vitamin K-dependent bone protein. Journal of Biological Chemistry 260:14971–14975.

[69] Jeffery, E., Berry, R., Church, C.D., Yu, S., Shook, B.A., Horsley, V., et al., 2014. Characterization of Cre recombinase models for the study of adipose tissue. Adipocyte 3:206–211.

[70] Gustafson, B., Smith, U., 2015. Regulation of white adipogenesis and its relation to ectopic fat accumulation and cardiovascular risk. Atherosclerosis 241:27–35.

[71] Qian, S.W., Liu, Y., Wang, J., Nie, J.C., Wu, M.Y., Tang, Y., et al., 2016. BMP4 cross-talks with estrogen/ERalpha signaling to regulate adiposity and glucose metabolism in females. EBioMedicine 11:91–100.

[72] Grefhorst, A., van den Beukel, J.C., van Houten, E.L., Steenbergen, J., Visser, J.A., Themmen, A.P., 2015. Estrogens increase expression of bone morphogenetic protein 8b in brown adipose tissue of mice. Biology of Sex Differences 6:7.

[73] Patil, M., Sharma, B.K., Satyanarayana, A., 2014. Id transcriptional regulators in adipogenesis and adipose tissue metabolism. Frontiers in Bioscience 19: 1386–1397.

[74] Patil, M., Sharma, B.K., Elattar, S., Chang, J., Kapil, S., Yuan, J., et al., 2017. Id1 promotes obesity by suppressing brown adipose thermogenesis and white adipose. Browning Diabetes 66:1611–1625.

